JOURNAL OF MATERIALS SCIENCE **35** (2000) 3181 – 3188

A comparison of sensitization kinetics in 304 and 316 stainless steels

E. ALMANZA, L. E. MURR
Department of Metallurgical and Materials Engineering and Materials Research Institute, The University of Texas at El Paso, El Paso, TX 79968, USA

The effects of tensile and cold rolling strain (up to 40%) over a range of grain sizes ranging from 300 μm to 10 μm on sensitization (and desensitization) were observed and compared for 304 and 316 stainless steel having a constant carbon content of 0.05%; at 670°C. Rapid sensitization-desensitization was observed for both materials at the smallest grain size, and plots of degree of sensitization (DOS) data with time, temperature, and tensile strain coupled with chromium diffusivity data for 304 stainless steel allowed activation energies to be calculated from corresponding Arrhenius plots utilizing supplemental data from Beltran, *et al.* [1] at 625°C and 775°C. Values of 1.9 and 2 kcal/mol were found for unstrained and 20% strained samples for 11 μm grain size while corresponding values at 175 μm grain size were 55 and 32 kcal/mol respectively. Activation energies for unstrained and 10% strained 316 stainless steel for 135 μm grain size were found to be 76 and 64 kcal/mol, respectively. Sensitization was more rapid for cold-rolling versus tensile straining in both stainless steels, and there was no detectable sensitization for the largest grain size regime of the 316 stainless steel up to 10 h aging time at 670°C. *© 2000 Kluwer Academic Publishers*

1. Introduction

In recent kinetic studies by Beltran, *et al.* [1], it was shown that when the grain size of 304 stainless steel was reduced from 150 μm to 15 μm, the sensitization kinetics were dramatically increased, and the time to sensitize and desensitize became so small as to be nearly instantaneous, especially at higher temperatures (∼775°C). In this context, both strain and strain state (simple tension versus biaxial straining or cold rolling) have also been shown to have a significant influence on carbide precipitation kinetics and the rate and character of corrosion sensitization, especially in 304 stainless steel [2–8]. Trillo and Murr [9] have also recently shown that a carbon threshold exists in 304 stainless steel. Below about 0.02% C there is essentially no sensitization or precipitation. Maldonado, *et al.* [10, 11] have recently demonstrated that carbide precipitation and sensitization are different in deformed (strained) 304 stainless steel in contrast to deformed 316 stainless steel (with essentially the same carbon content) because a high volume fraction of strain-induced (α') martensite in the 304 stainless steel [12, 13] can nucleate a 2-phase, α'/γ, fine-grained microstructure which promotes very rapid sensitization and precipitation of carbides, in contrast to 316 stainless steel where this 2-phase microstructure is considerably reduced or absent.

In the present study, we measure and compare the degree of sensitization (DOS) for a range of grain sizes and strains, as well as tension and rolling deformation; for 304 and 316 stainless steels at a constant carbon content (∼0.05% C). In addition, we have quantitatively evaluated the kinetics and diffusion mechanisms corresponding to DOS over a range of grain sizes, and measured the activation energies for sensitization and precipitation.

2. Experimental details

The austenitic 304 and 316 stainless steel compositions are given in Table I. A carbon content of nominally 0.05% C was consistent with optimum sensitization rates established in prior research [1, 8]. These alloy materials were received in mill-processed, 0.64 cm plate form, and sections were cut from these plates, cold rolled 70% and annealed at 1000°C for 1 minute to produce grain sizes of 11 μm and 10 μm for the 304 and 316 stainless steel respectively. These same plates were annealed at 1100°C for 1 h to produce an average grain size of 175 μm in the 304 stainless steel and at 1175°C for 2 h to produce a grain size of 110 μm in the 316 stainless steel. Finally, samples were annealed at 1300°C for 1.5 h to produce grain sizes of 300 and 280 μm in the 304 and 316 stainless steel, respectively. Grain sizes were measured utilizing the 3-circle Abrams procedure outlined in ASTM-E112-85 specifications [14]; using a 60% nitric acid electrolytic etch. This methodology was followed because it is consistent with electrochemical potentiokinetic reactivation (EPR) test procedures used to measure the degree of sensitization (DOS) described in detail in the earlier work of Beltran, *et al.* [1]. This included the test parameters described in Table II of reference [1] which were applied to both the 304 and 316 stainless steel samples in both the annealed conditions described above, and

TABLE I Chemical composition for 304 and 316 stainless steel

% wt	C	Cr	Ni	Mo	Mn
304 SS	0.05	18.31	8.08	0.35	1.60
316 SS	0.045	17.05	10.28	2.10	1.40

after straining by tensile testing to true strains of 20, 30, and 40 percent, and cold rolling to thickness strains of 20 and 40 percent.

After deformation processing, samples of both the 304 and 316 stainless steel were heat treated at 670°C for 0.1, 0.4, 1, 2, and 10 h and water quenched, and finally tested by single-loop EPR-DOS. Following EPR-DOS measurements, samples were observed by optical metallography to examine the intergranular and transgranular corrosion attack. Transmission electron microscopy (TEM) was also used to support EPR test results through selected examinations and documentation of carbide ($M_{23}C_6$) precipitation as described previously [1].

3. Results and discussion

3.1. Comparison of the effects of strain and grain size at 670°C

Fig. 1 shows for comparison the EPR-DOS values plotted as a function of aging times for 304 and 316 stainless steel deformed in tension, while Fig. 2 shows a corresponding comparison of EPR-DOS measurements for cold reduction by rolling; to equivalent strains and aging at 670°C. Consistent with earlier measurements for 304 stainless steel by Beltran, *et al.* [1] at 625 and 775°C, the uniaxially (tension) strained samples are observed to be fully sensitized earlier than the undeformed material as the grain size is reduced to 11 μm, and this is also true for the 316 stainless steel which exhibits considerably less sensitization overall on comparing the 10 μm grain size material. At the larger grain size end in Fig. 1, there is no sensitization for the 316 stainless steel in contrast to the 304 stainless steel. However, in the case of cold rolling, there is some sensitization in the 316 stainless steel for the highest strain (40%) and largest grain size, and the entire sensitization kinetics regime is accelerated in time for both the 304 and 316 stainless steel; as shown in Fig. 2. However, the sensitization kinetics are not much changed for the 304 and 316 stainless steel at the smallest grain sizes on comparing Figs 1 and 2, and this is generally consistent with the previous observations of Beltran, *et al.* [1] for 304 stainless steel deformed only in tension. However, the fact that both the strain and mode of straining does not significantly alter the kinetics in the 10 to 11 μm grain size range provides additional support for the overwhelming effect of grain boundary diffusion in the fine grain regime where this becomes dominant.

Fig. 3 shows for comparison the grain boundary carbides typical for sensitization in the 110 μm grain size 316 stainless steel strained 20% by rolling and the unstrained material; aged 10 h at 670°C as shown in the EPR-DOS data reproduced in Fig. 2. These observations are typical for those observed for 304 stainless steel in this work and in previous work [1]. The lack of sensitization after aging for 10 h in the unstrained condition is unambiguously demonstrated by the lack of carbides in the grain boundary in Fig. 3b.

3.2. Diffusivity and activation energy from DOS plots for 304 stainless steel

DOS is controlled by the $\sqrt{Dt}$ width of the chromium depleted zone. DOS-time from 0 to 120 C/cm^2 was considered diffusion dependent and in the 175 μm grain size material used to determine chromium diffusivity. For the case of the 10 μm grain size material, DOS-time from 0 to 5 C/cm^2 was considered diffusion dependent. Advani [15] developed an algorithm to evaluate the diffusivity of chromium as a function of strain in 316 stainless steel by comparing experimentally measured and theoretically predicted slopes of the DOS versus $\sqrt{t - t_0}$ data below 50 C/cm^2. The algorithm required as input the experimentally obtained DOS versus time (t) data and the time where DOS starts, t_0. The DOS values corresponding to times above t_0 were normalized with respect to t_0, and square root of the $(t - t_0)$ value was then computed. Linear regression of the DOS-$\sqrt{t - t_0}$ values was performed, and the slope of the curve was taken as the regression coefficient of the fitted line.

Theoretical slope determination involved a trial and error method. A diffusivity value was assumed by the algorithm and used to compute widths (W_{attk}) and the volume parameter (VP) of the chromium depletion at the chromium attack level, $\mathrm{Cr}_{\mathrm{attk}} = 13.5\%$ [16]. This is the critical Cr content where attack occurs in the EPR test. Since the chromium concentration is assumed to be constant along the grain boundary ($\mathrm{Cr}_{\mathrm{min.}}$) and no account is taken of the change in $M_{23}C_6$ composition with time, then the simplest way to treat the development of Cr-depletion profiles is to use the following solution to Fick's second law for diffusion [17]:

$$\frac{(\mathrm{Cr}_{\mathrm{attk}} - \mathrm{Cr}_{\mathrm{min}})}{(\mathrm{Cr}_{\mathrm{bulk}} - \mathrm{Cr}_{\mathrm{min}})} = \mathrm{erf}\left(\frac{W_{\mathrm{attk}}}{2\sqrt{D_{\mathrm{Cr}} t}}\right) \qquad (1)$$

Where $\mathrm{Cr}_{\mathrm{attk}}$ is the chromium attack level and $\mathrm{Cr}_{\mathrm{bulk}}$ is the chromium concentration in the bulk. D_{Cr} is the chromium diffusivity and t is the aging time. Equation 1 was used to compute widths at the attack level. The volume parameter (VP) of chromium depletion below 13.5% Cr level was evaluated by using the normalized equation [16]:

$$\mathrm{VP}_{13.5\%\mathrm{Cr}} = (\mathrm{Cr}_{\mathrm{attk}} - \mathrm{Cr}_{\mathrm{min}}) \times \frac{\mathrm{W}_{\mathrm{attk}}}{2\mathrm{Cr}_{\mathrm{attk}}} \qquad (2)$$

where VP represents the region of grain boundary chromium depletion below a critical level of chromium required for attack ($\mathrm{Cr}_{\mathrm{attk}} = 13.5\%$) in the EPR test. This equation was determined to investigate the combined effects of width and depth. The $\mathrm{Cr}_{\mathrm{min.}}$ value used in this computation for both 304 and 316 SS materials was taken as a direct output of the sensitization model developed by Bruemmer [16]. $\mathrm{Cr}_{\mathrm{min.}}$ was determined at the grain boundary using an analytical TEM fitted with an energy dispersive X-ray spectrometer (STEM-EDX). EPR-DOS values were consequently computed

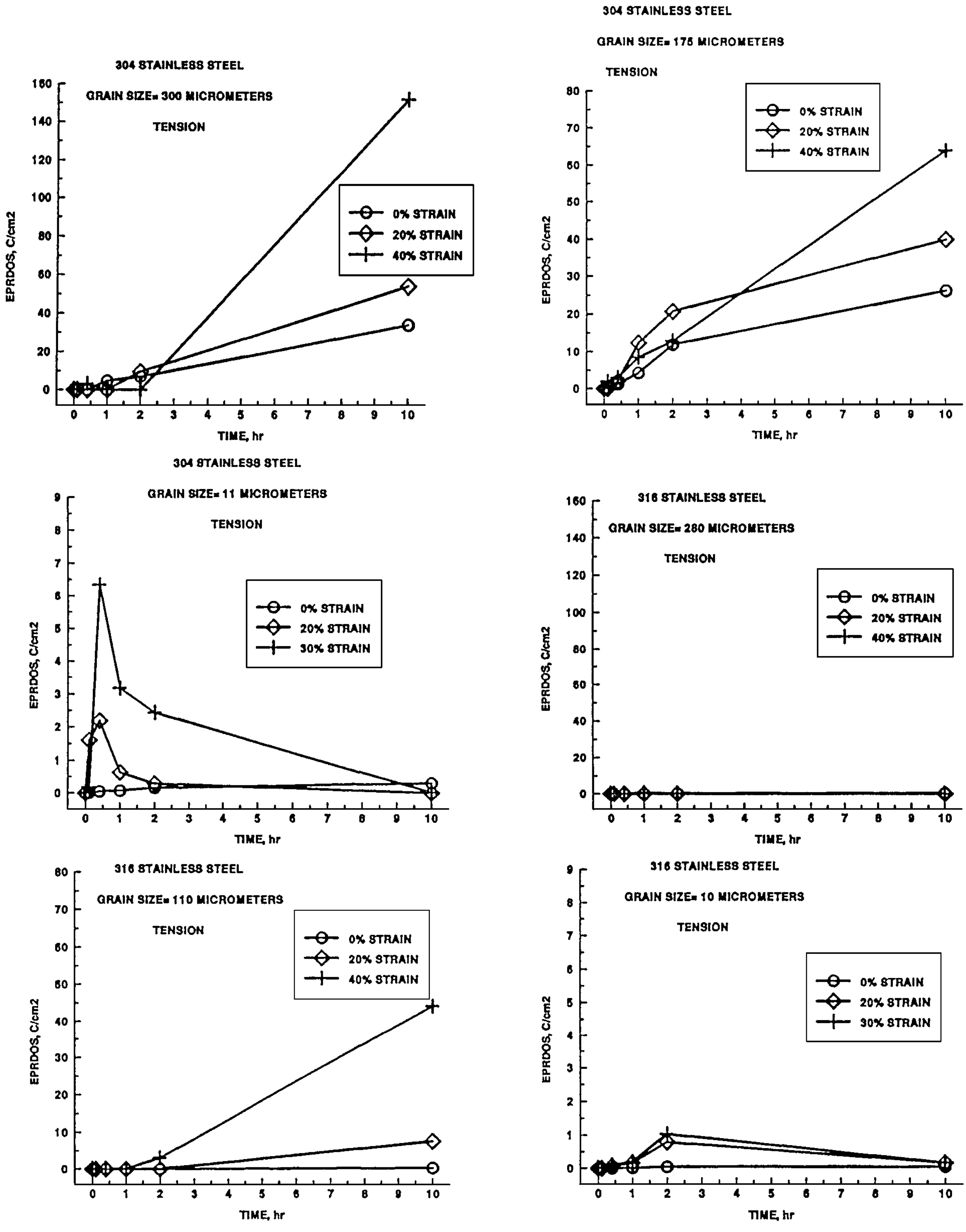

Figure 1 Comparison of EPR-DOS (sensitization) curves for type 304 and 316 stainless steels deformed at strains shown in tension, for a range of grain sizes; aged at 670°C.

using the correlation between DOS and VP [16]:

$$\text{ERP-DOS} = 1.1\text{VP} - 6.1 \times 10^{-3}\,\text{VP}^2 + 1.3 \times 10^{-5}\,\text{VP}^3 \qquad (3)$$

Equation 3 was obtained when DOS values were related to STEM-EDX measurements of grain boundary chromium depletion [16]. Each calculation was carried out for a series of time values at each diffusivity, and slopes of the EPR-DOS versus $\sqrt{t}$ were compared with those obtained in the experiment, until a diffusivity value that provided identical slopes as the experiment was obtained by the algorithm. Fig. 4a depicts the effect on EPR slope as a function of temperature for 304 SS samples strained by tension; with a grain size of 175 μm. This illustrates that the slope increases systematically from 4 C/cm^2/$\sqrt{h}$ to 9.9 C/cm^2/$\sqrt{h}$ at 625°C in samples strained by tension from 0% to 20%

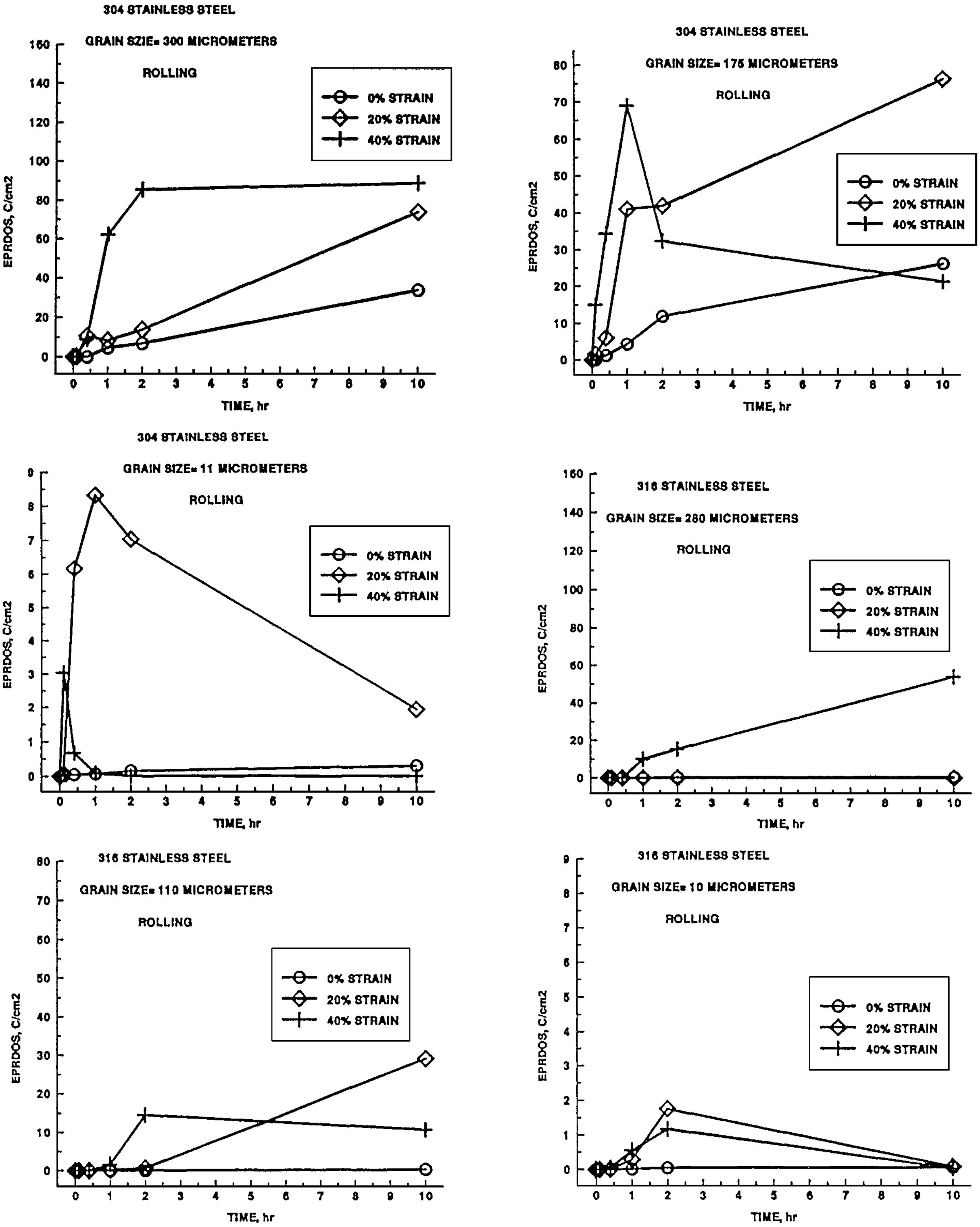

Figure 2 Comparison of EPR-DOS (sensitization) curves for type 304 and 316 stainless steels deformed at cold-rolling reductions (strains) shown for a range of grain sizes corresponding to Fig. 1; aged at 670°C.

in the work of Beltran [1, 18]. An increase in slope is also observed at 670°C (this work). In the slope data at 775°C from Beltran [1, 18] there is no systematic correlation between slope and strain since the slope is not dramatically affected as in the case of the two other temperatures. Conversion of the slope data to diffusivity, Fig. 4b, yields trends similar to those observed in Fig. 4a. At 625°C the diffusivity increases by about an order of magnitude from 1.3×10^{-16} cm^2/sec to 1.2×10^{-15} cm^2/sec with increasing strain from 0% to 20%. Also, an increase in the diffusivity at 670°C is observed, but the magnitude of this increase is only a factor of about 4 for the same strain levels. On the other hand, at 775°C the diffusivity is relatively constant at 1.0×10^{-14} cm^2/sec for 0% and 20% strain levels. The results shown in Fig. 4b reveal that the effect of strain on the sensitization kinetics is to enhance the rate of sensitization (Cr-diffusivity), as would be expected.

Utilizing diffusivity data implicit in Fig. 4b and corresponding data for the 11 μm grain size material for the current work along with prior data of Beltran [1, 18],

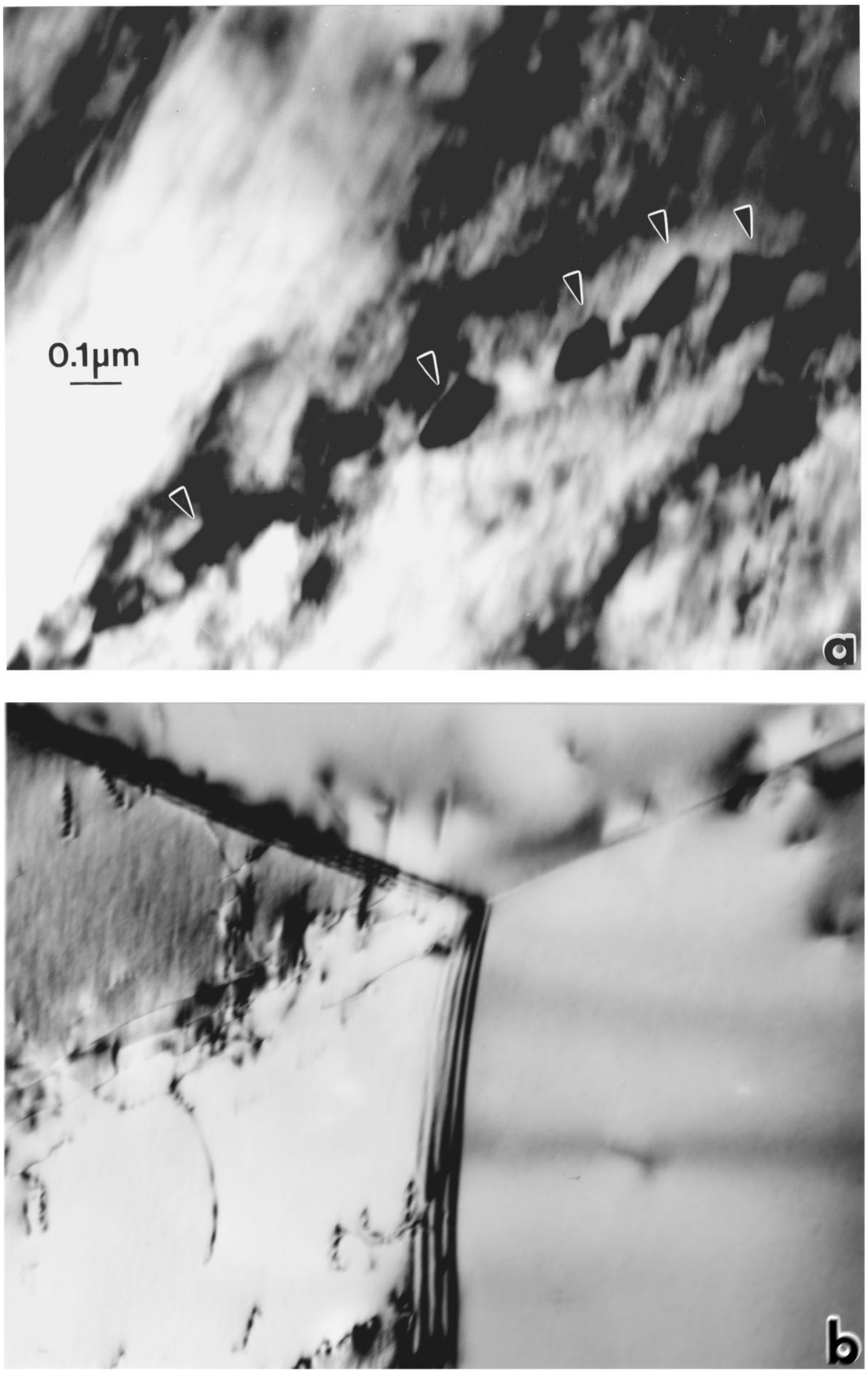

Figure 3 TEM bright-field images for 316 stainless steel. (a) cold rolled 20% and aged 10 h at 670°C showing grain boundary precipitates (arrows). (b) unstrained sample aged 10 h at 670°C showing grain boundaries free of precipitates. The grain size was 110 μm (see Fig. 2).

TABLE II Experimental activation energies (Q_a) for 304 stainless steel as a function of strain and grain size

	Activation energy (kcal/mol)	
Grain size (μm)	0%ε	20%ε
11	1.9	2.0
175	55.1	32.2

an Arrhenius plot was constructed as shown in Fig. 5. Corresponding activation energies, Q_a, were then calculated from the corresponding slopes as shown in Table II. These values provide quantitative comparisons for the rather dramatic sensitization kinetic differences which are characteristic of the medium-to-large grain size stainless steels ($\geq$175 μm) in contrast to small grain sizes ($\leq$11 μm).

Differences in sensitization (Cr-diffusivity) kinetics with increasing strain have been postulated to be due to increased dislocation density with strain which in turn enhances dislocation pipe diffusion of chromium. The Hart [19] dislocation pipe diffusion equation in the general form:

$$D_{\mathrm{tot}} = D_0 \exp\left(\frac{-Q_{\mathrm{a}}}{RT}\right) + \rho A D_{0,\mathrm{p}} \exp(-Q_{\mathrm{a,p}}/RT) \tag{4}$$

indicates that the total diffusivity (D_{tot}) in strained materials increases with increasing dislocation density (ρ).

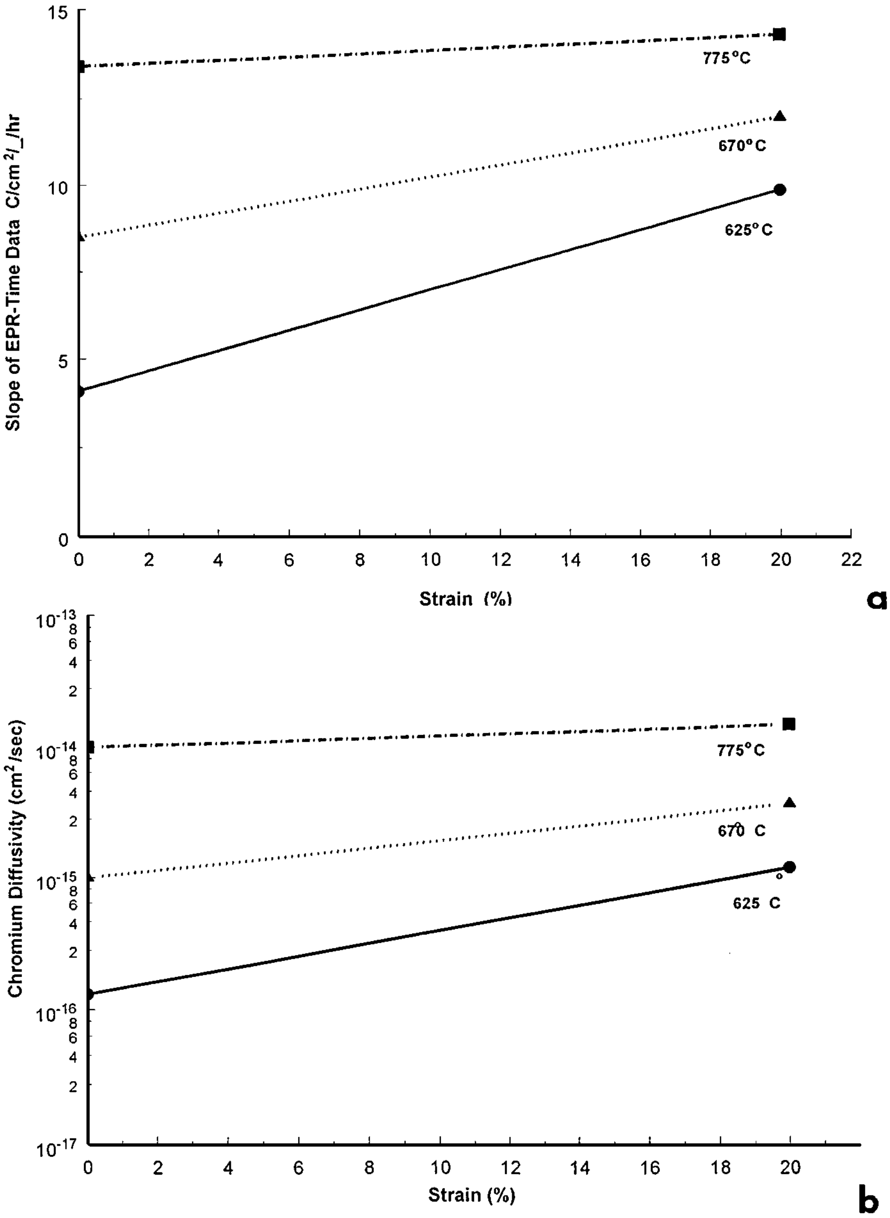

Figure 4 Comparison of the effects of strain in EPR-DOS slope for 175 μm grain size 304 stainless steel as a function of aging temperature (a) and chromium diffusivity prediction from the EPR-DOS slopes (b). Magnification for (a) and (b) shown in (a).

This yields higher diffusivities in samples strained to higher levels. Note in Equation 4 that D_0 is the initial, bulk diffusivity, Q_a is the corresponding activation energy, R is the gas constant, and T is the absolute temperature. $D_{0,p}$ is a new diffusivity while A is a constant and $Q_{a,p}$ is the activation energy associated with dislocation diffusion. Although the documentation of the specific increases of the Cr-diffusivity by the dislocation pipe diffusion model has not been made in this work, direct observations of this issue made by Advani [15] and Andresen *et al.* [19] support this result for the 316 stainless steel material. Therefore, the mechanism by which sensitization development occurs in a 304 stainless steel with a grain size of 175 μm is also controlled by dislocation pipe diffusion. Experimental data for activation energies (Q_a) for 316 stainless steel samples strained by tension 0% to 16% having a 135 μm grain size are given in Table III [15]. This implies that with increasing strain the activation energy (Q_a) decreases as was observed in the 304 stainless steel samples (see Table II). The decrease of Q_a in both materials is an indication that strain accelerates sensitization development. On the other hand, the larger Q_a in 316 stainless steel in contrast to the 304 stainless steel confirms the fact that diffusion occurs faster in 304 stainless steel. Since the activation energy decreases as the strain increases in both 304 and 316 stainless steel, it suggests that the mechanism by which sensitization development occurs in both materials is controlled by dislocation pipe diffusion in medium-to-large grain sizes.

It can be noted on comparing Tables II and III that the activation energies for diffusion for 304 and 316 stainless steels at corresponding strains (or in the unstrained condition specifically) in the grain size range of ~175 μm to 135 μm vary by nearly a factor 2 in the strained condition. This probably applies to the very small grain size regime as well if we examine Figs 1 and 2 retrospectively, for 11 μm and 10 μm grain size regimes for the 304 and 316 stainless steel respectively.

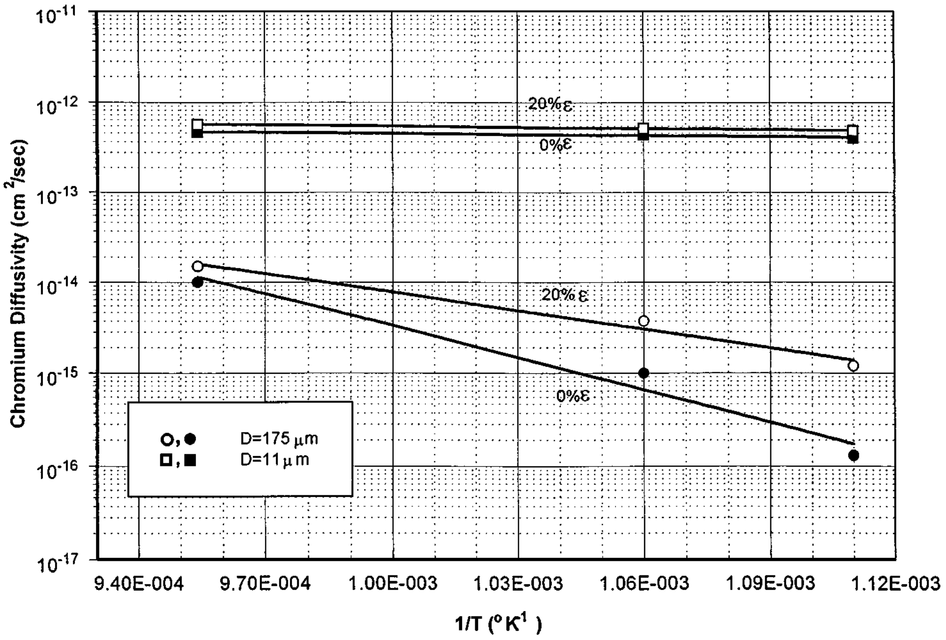

Figure 5 Arrhenius plot of log diffusivity versus inverse (absolute) temperature for 304 stainless steel unstrained samples and samples trained in tension by 20%; having grain sizes of 11 μm and 175 μm respectively.

TABLE III Experimental data for activation energies (Q_a) for 316 stainless steel samples strained by tension; with a grain size of 135 μm

Strain (%)	Activation energy (kcal/mol)
0	76
2	74
6	65
10	64
16	62

4. Summary and conclusions

This research program has compared the sensitization behavior of 0.05% C 304 and 316 stainless steels and generally confirmed previous conclusions regarding the effect of decreasing grain size, deformation (or strain) as well as the mode of deformation on the sensitization-desensitization kinetics [1]; at 670°C. In addition, this study has provided quantitative evidence for these kinetic features, and activation energies have been calculated from Arrhenius and related representations of sensitization data and diffusional phenomena. The mechanisms of diffusion implicit in prior studies in going from larger grain sizes of around 10^2 μm to 10 μm were validated in this study on 304 stainless steel by activation energies of 1.9 kcal/mol and 2.0 kcal/mol for strains of 0 and 20% respectively for grain sizes of ∼10 μm; in contrast to activation energies of 55.1 and 32.2 kcal/mol for the same, corresponding strains, and a grain size of 175 μm. For grain sizes around 135 μm, activation energies of 76 and 62 kcal/mol were obtained for 316 stainless steel strained 0 and 16% respectively. Consequently, in the 10^2 μm grain size range, the activation energies for Cr diffusion were roughly twice as large in 316 stainless steel in contrast to 304 stainless steel; at essentially the same strain values.

A comparison of degree of sensitization (DOS) values for both tension and rolling deformation in 304 and 316 stainless steel along with corresponding desensitization showed a more pronounced effect for rolling deformation in contrast to tension, and the sensitization in both stainless steels was accelerated as the grain size was reduced; following the trend of activation energies noted above. For larger grain sizes of 280 μm, the 316 stainless steel did not exhibit any sensitization after 10 h aging at 670°C while at the smallest grain size of 11 μm, the 304 stainless steel sensitized in a few minutes when aged at 670°C.

Acknowledgements

This research was supported in part by U.S. Department of Defense Logistics Agency (DLA) Defense National Stockpile Center Grant DN-009, a Conacyt (Mexico) Graduate Scholarship and the Instituto Tecnologico de Saltillo, Saltillo Mexico.

References

1. R. BELTRAN, J. G. MALDONADO, L. E. MURR and W. W. W. FISHER, *Acta Mater.* **45**(10) (1997) 4351.
2. C. L. BRIANT and A. M. RITTER, *Scripta Metall.* **13** (1979) 177.
3. *Idem.*, *Metall. Trans.* **11A** (1981) 910.
4. A. BOSE and P. K. DE, *Corrosion* **43** (1987) 624.
5. L. E. MURR, A. H. ADVANI, S. SHANKAR and D. G. ATTERIDGE, *Mater. Characterization* **24** (1990) 135.
6. A. H. ADVANI, L. E. MURR, D. G. ATTERIDGE, R. CHELAKARA and S. M. BRUEMMER, *Corrosion* **47** (1991) 939.
7. A. H. ADVANI, L. E. MURR, D. G. ATTERIDGE and R. CHELAKARA, *Metall. Trans.* **22A** (1991) 2917.
8. E. A. TRILLO, R. BELTRAN, J. G. MALDONADO, R. J. ROMERO, L. E. MURR, W. W. FISHER and A. H. ADVANI, *Mater. Characterization* **35** (1995) 99.
9. E. A. TRILLO and L. E. MURR, *Acta Mater.* **47**(1) (1998) 235.
10. J. G. MALDONADO, A. H. ADVANI, L. E. MURR and W. W. FISHER, in "Microstructural Science, Vol. 21," edited by

C. R. Brooks and M. R. Louthan, Jr. (ASM International, Materials Park, OH, 1994) p. 23.
11. J. G. MALDONADO, L. E. MURR and W. W. FISHER, in Iron and Steel Society Proceedings, 37th MWSP Conf. Proc., ISS XXXIII, 1996, p. 849.
12. L. E. MURR, K. P. STAUDHAMMER and S. S. HECKER, *Metall. Trans.* **13A** (1982) 627.
13. K. P. STAUDHAMMER, L. E. MURR and S. S. HECKER, *Acta Metall. et Materialia* **33** (1983) 267.
14. Standard test method for determining average grain size, Annual Book of Standards, 3.01 (E112-88) (American Society for Testing Materials, Philadelphia, PA, 1988).
15. A. H. ADVANI, Ph.D. dissertation, Oregon Graduate Institute, Portland, OR, 1989.
16. S. M. BRUEMMER, Ph.D. dissertation, Oregon Graduate Institute, Portland, OR, 1988.
17. T. THORVALDASSON and A. SALWEN, *Scripta Metall.* **18** (1984) 739.
18. R. BELTRAN, M.S. thesis, The University of Texas at EI Paso, EI Paso, TX, 1996.
19. P. L. ANDRESEN, D. D. SOLOMON and D. F. TAYLOR, EPRI NP-1823, Project 1072-1 (Final Report), Electric Power Research Institute, Palo Alto, CA, May, 1981.

Received 15 November
and accepted 14 December 1999